Endocrinology, Diabetes & Metabolism CASE REPORTS

S Kawai and others | Effective localization in TIO

ID: 17-0005; April 2017
DOI: 10.1530/EDM-17-0005

Effective localization in tumor-induced osteomalacia using ^{68}Ga-DOTATOC-PET/CT, venous sampling and 3T-MRI

Shintaro Kawai[1], Hiroyuki Ariyasu[1], Yasushi Furukawa[1], Reika Yamamoto[1], Shinsuke Uraki[1], Ken Takeshima[1], Kenji Warigaya[2], Yuji Nakamoto[3] and Takashi Akamizu[1]

[1]The First Department of Medicine, [2]Department of Human Pathology, Wakayama Medical University, Wakayama, Japan, and [3]Department of Diagnostic Imaging and Nuclear Medicine, Kyoto University Graduate School of Medicine, Kyoto, Japan

Correspondence should be addressed to H Ariyasu
Email
ariyasu@wakayama-med.ac.jp

Summary

Tumor-induced osteomalacia (TIO) is a rare paraneoplastic syndrome characterized by renal phosphate wasting leading to hypophosphatemia due to excessive actions of fibroblast growth factor 23 (FGF23) produced by the tumors. Although the best way of curing TIO is complete resection, it is usually difficult to detect the culprit tumors by general radiological modalities owing to the size and location of the tumors. We report a case of TIO in which the identification of the tumor by conventional imaging studies was difficult. Nonetheless, a diagnosis was made possible by effective use of multiple modalities. We initially suspected that the tumor existed in the right dorsal aspect of the scapula by ^{68}Ga-DOTATOC positron emission tomography/computed tomography (^{68}Ga-DOTATOC-PET/CT) and supported the result by systemic venous sampling (SVS). The tumor could also be visualized by 3T-magnetic resonance imaging (MRI), although it was not detected by 1.5T-MRI, and eventually be resected completely. In cases of TIO, a stepwise approach of ^{68}Ga-DOTATOC-PET/CT, SVS and 3T-MRI can be effective for confirmation of diagnosis.

Learning points:

- TIO shows impaired bone metabolism due to excessive actions of FGF23 produced by the tumor. The causative tumors are seldom detected by physical examinations and conventional radiological modalities.
- In TIO cases, in which the localization of the culprit tumors is difficult, ^{68}Ga-DOTATOC-PET/CT should be performed as a screening of localization and thereafter SVS should be conducted to support the result of the somatostatin receptor (SSTR) imaging leading to increased diagnosability.
- When the culprit tumors cannot be visualized by conventional imaging studies, using high-field MRI at 3T and comparing it to the opposite side are useful after the tumor site was determined.

Background

Tumor-induced osteomalacia (TIO) is a paraneoplastic syndrome characterized by renal phosphate wasting leading to hypophosphatemia due to excessive actions of fibroblast growth factor 23 (FGF23) produced by the tumor (1, 2). TIO is a rare disease and while more than 300 cases have been reported in the literature since the association between renal phosphate wasting and the presence of tumors was first made, the prevalence

ID: 17-0005; April 2017
DOI: 10.1530/EDM-17-0005

is not well known (3). Most FGF23 producing tumors are benign mesenchymal tumors, whose pathological features are classified as phosphaturic mesenchymal tumor with mixed connective tissue variant (PMTMCT) (4). The best way of curing TIO is complete resection. However, it is typically difficult by means of general radiological modalities to detect the culprit tumors because they are usually too small in size; they grow slowly and exist in the bones. When the tumors cannot be detected, medication must be chosen as a symptomatic treatment. However, improvement of symptoms and hypophosphatemia is often partial and the controlling of serum phosphate frequently needs a large amount of medication for a long time. As a result, adverse events, such as hyperparathyroidism, nephrocalcinosis and nephrolithiasis may arise (5). Therefore, as many examinations to detect the causative tumors as possible should be performed and further improvement in the diagnostic process of TIO whose cases are hard to localize is needed. Herein, we report a case of TIO in which it was difficult to identify the culprit tumor both functionally and anatomically by conventional modalities. Nonetheless,

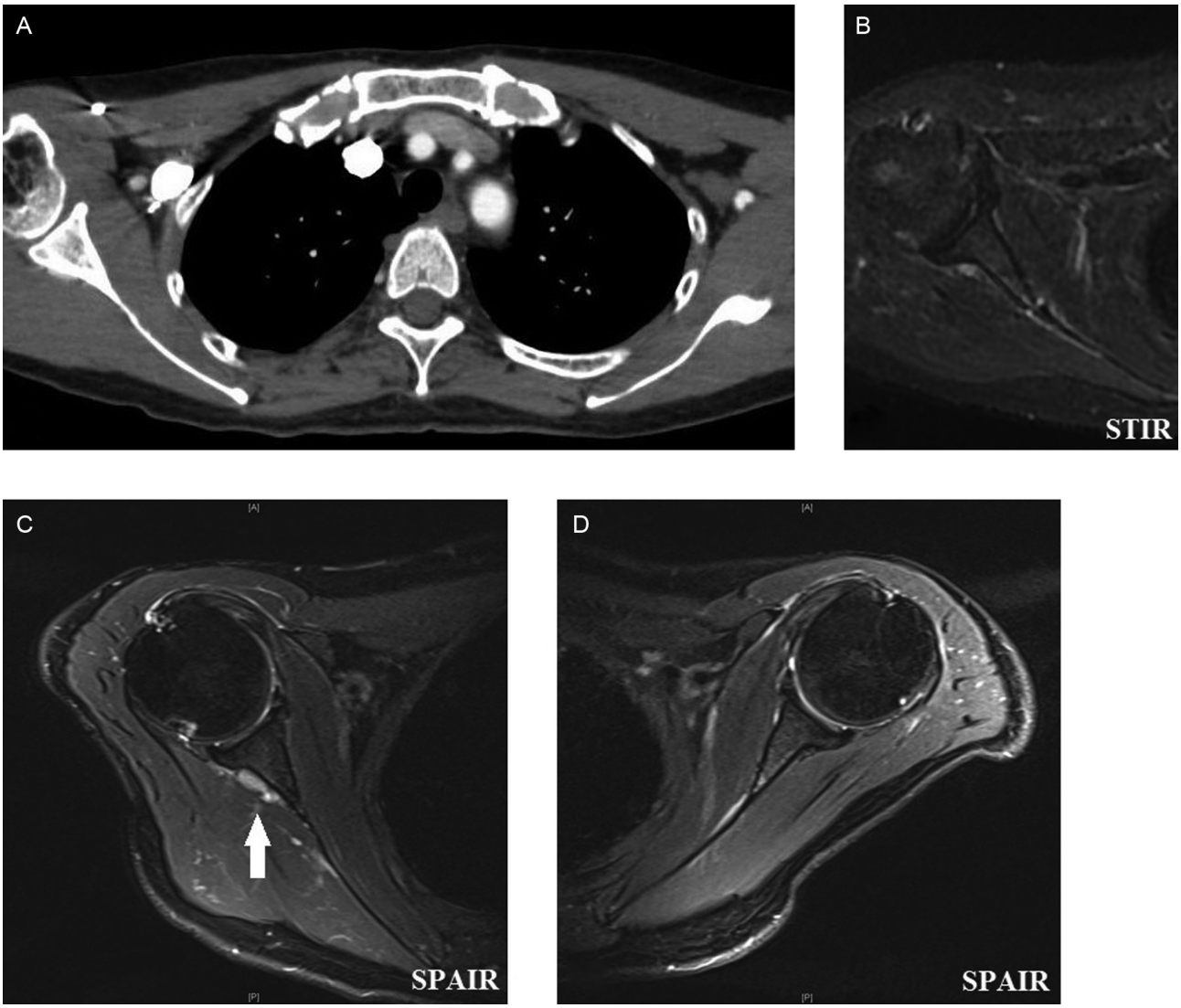

Figure 1
Conventional imaging studies and 3T-MRI. (A) CECT undertaken as a screening for malignancy. Compared with the result of ^{68}Ga-DOTATOC-PET/CT (Fig. 2), the right dorsal scapula was more enhanced than the left. (B) 1.5T-MRI of the right shoulder joint. No tumors could be identified as clear lesions. (C) 3T-MRI of the right shoulder joint. It revealed a small nodule measuring 10×4 mm on the right dorsal scapula which is the site ^{68}Ga-DOTATOC uptake. (D) 3T-MRI of the left shoulder joint. No nodular lesions were detected in the left side. 251×213 mm (96×96 DPI).

ID: 17-0005; April 2017
DOI: 10.1530/EDM-17-0005

Table 1 Laboratory data on admission.

Parameters	Values	Reference range
Albumin, g/dL	4.4	3.9–4.9
ALP, IU/L	1,135	120–370
BUN, IU/L	18	8–20
Creatinine, mg/dL	0.50	0.43–0.72
UA, mg/dL	3.8	2.4–5.6
Sodium, mEq/L	142	135–145
Potassium, mEq/L	3.6	3.5–5.0
Chloride, mEq/L	105	98–107
Calcium, mg/dL	9.0	8.7–11.0
Phosphate, mg/dL	1.6	2.5–4.5
BAP, IU/L	133.4	3.7–20.9
25(OH) D, ng/mL	9	15–40
Intact PTH, pg/mL	111	10–65
FGF23, pg/mL	43	10–50
%TRP, %	70.7	80–94

*ALP, alkaline phosphatase; BUN, blood urea nitrogen; UA, uric acid; BAP, bone alkaline phosphatase; PTH, parathormone; FGF, fibroblast growth factor; TRP, tubular reabsorption of phosphate

a final diagnosis was reached by using ^{68}Ga-DOTATOC positron emission tomography/computed tomography (^{68}Ga-DOTATOC-PET/CT), systemic venous sampling (SVS) and 3T-magnetic resonance imaging (MRI).

Case presentation

A 53-year-old female was admitted to a hospital with bone pain in the limbs, rib cage and buttocks for half a year. Laboratory data showed elevated alkaline phosphatase (ALP) of 1135 IU/L. Bone scintigraphy revealed increased radiotracer uptake in the calcaneus, rib cage and buttocks. At first, bone metastasis was suspected, but whole body contrast-enhanced CT (CECT) (Fig. 1A), 1.5T-MRI (Fig. 1B) and endoscopic examination detected no malignant tumors. The patient was referred to our hospital for further investigation. Laboratory data on admission showed severe hypophosphatemia, and the percentage of

Figure 2
^{68}Ga-DOTATOC-PET/CT. PET/CT imaging showed elevated uptake of ^{68}Ga-DOTATOC on the right dorsal aspect of the scapula (SUVmax: 4.9).

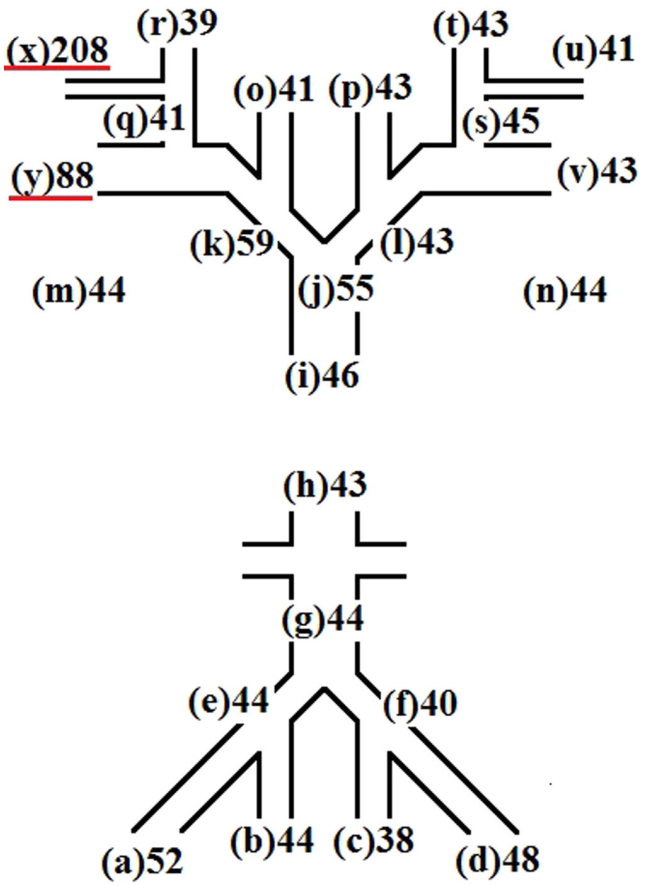

Figure 3
Systemic venous sampling for FGF23. Venous blood samples were collected from various veins as listed above. Each value represents FGF23 levels in these portions (pg/mL). The levels were markedly elevated in the right peripheral veins of the scapula, such as (x) and (y). (a) right external iliac vein, (b) right internal iliac vein, (c) left internal iliac vein, (d) left external iliac vein, (e) right common iliac vein, (f) left common iliac vein, (g) inferior vena cava (distal), (h) inferior vena cava (proximal), (i) superior vena cava (proximal), (j) superior vena cava (distal), (k) right brachiocephalic vein, (l) left brachiocephalic vein, (m) right brachial vein, (n) left brachial vein, (o) right internal jugular vein, (p) left internal jugular vein, (q) right external jugular vein (proximal), (r) right external jugular vein (distal), (s) left external jugular vein (proximal), (t) left external jugular vein (distal), (u) left suprascapular vein, (v) left axillary vein, (x) right suprascapular vein and (y) right axillary vein. 105 × 158 mm (96 × 96 DPI).

tubular reabsorption of phosphate was decreased at 70.7% (reference range: 80–94%), reflecting renal phosphate wasting (Table 1). Dual energy X-ray absorptiometry scan showed low bone mineral density. These results indicated that the patient was suspected with osteomalacia. She did not have any family history of metabolic bone disease. Serum level of FGF23 was 43 pg/mL and was thought to be notably high in hypophosphatemia. Based on these results, a diagnosis of TIO was highly probable. However, physical examination was otherwise normal, except for an occipital subcutaneous nodule of 1 cm in diameter.

ID: 17-0005; April 2017
DOI: 10.1530/EDM-17-0005

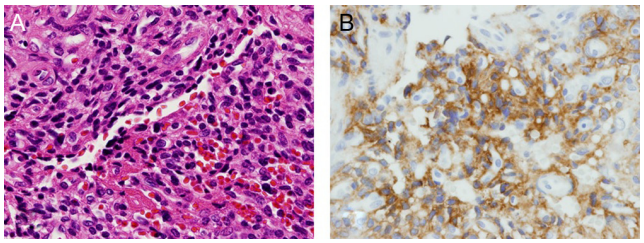

Figure 4
Histological analyses of the resected tumor. (A) Hematoxylin and eosin staining sections. Proliferation of spindle cells, which was consistent with PMTMCT, was seen. (B) Immunohistochemistry for SSTR2. SSTR2 staining was diffusely positive. 230 × 84 mm (96 × 96 DPI).

Whole body ^{18}F-fluorodeoxyglucose PET/CT (^{18}F FDG-PET/CT) scan showed intense uptake in the rib, hip and heel bones where bone scintigraphy was identified, but no tumor lesions were detected (data not shown).

Investigation

For further investigation, ^{68}Ga-DOTATOC-PET/CT was performed, and the imaging showed elevated uptake of ^{68}Ga-DOTATOC in the right dorsal aspect of the scapula (Fig. 2), but not in the limbs, rib cage, buttocks or the occipital subcutaneous nodule. To assess the validity of this result, systemic venous sampling (SVS), including some veins around the scapula, was conducted. Serum FGF23 level in the right suprascapular vein, the most proximal vein to the ^{68}Ga-DOTATOC uptake site, was markedly higher than those in any other vein (Fig. 3). These results strongly suggested that the FGF23-producing tumor existed in the right dorsal scapula. As a preparation for surgery, bilateral 3T-MRI of the shoulder was carried out. It revealed a small nodule of 10 × 4 mm in the right dorsal aspect of the scapula (Fig. 1C) and that was not detected in the left side (Fig. 1D). Based on these findings, we confirmed that this tumor was responsible for TIO. Although this lesion was not highlighted in the first survey using CECT and 1.5T-MRI, by retrospectively comparing with the images of ^{68}Ga-DOTATOC-PET/CT and 3T-MRI, the right dorsal scapula seemed to be more enhanced than the left in the CECT image (Fig. 1A). However, the images of CECT were not clear enough to locate the tumor's position and size.

Treatment

We suggested the patient to undergo surgery at the soonest possibility. However, she refused immediately. Therefore, we initiated treatment with dibasic sodium phosphate anhydrous and 1,25-$(OH)_2$ vitamin D alphacalcidol to maintain serum levels of phosphate and calcium. Consequently, serum ALP level was decreased, and phosphate level was increased and both were normalized in the preoperative period. However, the dosages of dibasic sodium phosphate anhydrous were increased (to 2100 mg/day as phosphate). Therefore, adverse events, such as hyperparathyroidism, nephrocalcinosis and nephrolithiasis, were of concern. Bone pain also persisted, although there was an improvement. The percentage of tubular reabsorption of phosphate remained low, indicating that the overproduction of FGF23 from the culprit tumor persisted. Thereafter, tumorectomy was performed using intraoperative portable CT.

Outcome and follow-up

Medication was stopped prior to surgery. On postoperative day five, serum level of FGF23 decreased to 20 pg/mL and the percentage of tubular reabsorption of phosphate improved to 94.2%. Histological features of the resected tumor were compatible with those in PMTMCT (Fig. 4A) and in immunohistochemistry for SSTR2. Positive cells were seen diffusely (Fig. 4B), supporting the diagnosis. After half a year from the operation, hypophosphatemia and corresponding symptoms such as bone pain have not recurred without any medication.

Discussion

In the present case, we were able to exactly localize the causative tumor by effectively using multiple diagnostic modalities and finally cured our patient from TIO. Only a few cases of TIO have been reported but the best diagnostic process is a challenging problem. It is important to localize the tumors responsible for TIO, taking full advantage of each modality.

^{68}Ga-DOTATOC-PET/CT should be at first conducted as a screening of localization of the culprit tumors when they cannot be detected by conventional radiological modalities, such as plain CT, MRI or ^{18}F FDG-PET/CT. Somatostatin receptor (SSTR) 2A is highly expressed in PMTMCT, which is a typical histological feature in the majority of TIO patients (6). In the diagnosis of neuroendocrine tumors, which also often express SSTR, ^{111}In-pentetreotide single-photon emission computed tomography/CT (Octreoscan-SPECT/CT) is frequently undertaken. Moreover, in recent years a new generation of SSTR imaging, PET/CT using ^{68}Ga-radiolabeled DOTA-

ID: 17-0005; April 2017
DOI: 10.1530/EDM-17-0005

conjugated peptide including DOTATOC, DOTATATE and DOTANOC is becoming available. Since DOTA-peptides selectively bind to SSTR2 (7), in the diagnosis of TIO, the use of this functional imaging apparatus is spreading globally. El-Maouche *et al*. reported the prospective study comparing ^{68}Ga-DOTATATE-PET/CT to Octreoscan-SPECT/CT and ^{18}F FDG-PET/CT in TIO localization. The sensitivity and specificity of ^{68}Ga-DOTATATE-PET/CT was 54.5% and 85.7%; Octreoscan-SPECT/CT, 36.3% and 80% and ^{18}F FDG-PET/CT, 36.3% and 86% respectively, showing high diagnosability of PET/CT using ^{68}Ga-DOTA-peptide for TIO (8). Since the prospective study of the sensitivity and specificity of ^{68}Ga-DOTATOC-PET/CT on TIO has not been reported, partly because of its rarity, there are only a few case reports (7, 9). In our case, immunohistochemistry for SSTR2 on the resected tumor showed positive staining; therefore, the sensitivity and specificity of ^{68}Ga-DOTATOC-PET/CT may be equal to or higher than that of ^{68}Ga-DOTATATE-PET/CT. Further large-scale studies are needed to validate ^{68}Ga-DOTATOC-PET/CT.

SVS is thought to be effective as a supporting method to localize the culprit tumors. Although some reports referred to the usefulness of SVS (10, 11), there was only one case of the tumor responsible for TIO being localized by SVS alone (12). Ito *et al*. conducted a prospective study of 10 patients with suspected TIO whose culprit tumors had not been detected by conventional imaging modalities (13). In this study, SVS was first performed and then CT or MRI was conducted based on the result of SVS. In eight out of ten patients, the tumor could finally be identified; however, it was only in four patients that the maximum point of FGF23 was in accordance with the site the tumor existed. These results suggest that SVS may be inappropriate for the screening of localization of FGF23-producing tumors. However, like our case, a combination of SVS and ^{68}Ga-DOTATOC-PET/CT should provide a precise diagnosis of TIO.

The tumors responsible for TIO are usually very small and exist in the bone. Thus, they cannot be frequently visualized by conventional radiological modalities. Signal-to-noise ratio of 3T-MRI increases to approximately twice that of 1.5T-MRI and the spatial image resolution improves. As a result, high quality images are visualized in the musculoskeletal system (14). Therefore, 3T-MRI is more useful for the detection of small tumors than 1.5T-MRI. In the detection of culprit tumors causing osteomalacia, the validity of 3T-MRI compared with 1.5T-MRI has not been established. In the present case, by conducting bilateral 3T-MRI of the shoulder, and additionally by comparing the right side to the left, we could visualize the small lesion. 3T-MRI has the disadvantage that, in moving internal organs, artifacts tend to affect the diagnostic quality since imaging time to obtain good contrast becomes longer due to the extension of the relaxation time. However, in the cases of TIO, tumors are static because they usually exist in the bone. This advantage does not need to be considered. Therefore, 3T-MRI is thought to be a useful modality as the preoperative inspection for surgical treatment of TIO.

In conclusion, a stepwise approach of ^{68}Ga-DOTATOC-PET/CT, SVS and 3T-MRI can be effective for the confirmation of diagnosis of TIO.

Declaration of interest
The authors declare that there is no conflict of interest that could be perceived as prejudicing the impartiality of the research reported.

Funding
This research did not receive any specific grant from any funding agency in the public, commercial or not-for-profit sector.

Patient consent
Written informed consent has been obtained from the patient for publication of this case report.

Author contribution statement
S Kawai is an endocrinologist physician who followed the patient during her hospitalization and wrote the first draft. H Ariyasu is also an endocrinologist physician and is responsible for case description. Y Furukawa is an endocrinologist physician following the patient at present. R Yamamoto, S Uraki and K Takeshima are endocrinologist physicians who followed the patient during her hospitalization. K Warigaya performed the histology analysis. Y Nakamoto conducted ^{68}Ga-DOTATOC-PET/CT. T Akamizu is the director of the First Department of Medicine and revised and approved the final draft.

References

1 Drezner MK 2001 Tumor-induced osteomalacia. *Reviews in Endocrine and Metabolic Disorders* **2** 175–186. (doi:10.1023/A:1010006811394)
2 Fukumoto S 2014 Diagnostic modalities for FGF23-producing tumors in patients with tumor-induced osteomalacia. *Endocrinology and Metabolism* **29** 136–143. (doi:10.3803/EnM.2014.29.2.136)
3 Dadoniene J, Miglinas M, Miltiniene D, Vajauskas D, Seinin D, Butenas P & Kacergius T 2016 Tumor-induced osteomalacia: a literature review and a case report. *World Journal of Surgical Oncology* **14** 4. (doi:10.1186/s12957-015-0763-7)
4 Folpe AL, Fanburg-Smith JC, Billings SD, Bisceglia M, Bertoni F, Cho JY, Econs MJ, Inwards CY, Jan de Beur SM, Mentzel T, *et al*. 2004 Most osteomalacia-associated mesenchymal tumors are a single

histopathologic entity: an analysis of 32 cases and a comprehensive review of the literature. *American Journal of Surgical Pathology* **28** 1–30. (doi:10.1097/00000478-200401000-00001)

5 Tarasova VD, Trepp-Carrasco AG, Thompson R, Recker RR, Chong WH, Collins MT & Armas LAG 2013 Successful treatment of tumor-induced osteomalacia due to an intracranial tumor by fractionated stereotactic radiotherapy. *Journal of Clinical Endocrinology and Metabolism* **98** 4267–4272. (doi:10.1210/jc.2013-2528)

6 Houang M, Clarkson A, Sioson L, Elston MS, Clifton-Bligh RJ, Dray M, Ranchere-Vince D, Decouvelaere AV, de la Fouchardiere A & Gill AJ 2013 Phosphaturic mesenchymal tumors show positive staining for somatostatin receptor 2A (SSTR2A). *Human Pathology* **44** 2711–2718. (doi:10.1016/j.humpath.2013.07.016)

7 Maybody M, Grewal RK, Healey JH, Antonescu CR, Fanchon L, Hwang S, Carrasquillo JA, Kirov A & Farooki A 2016 Ga-68 DOTATOC PET/CT-guided biopsy and cryoablation with autoradiography of biopsy specimen for treatment of tumor-induced osteomalacia. *CardioVascular and Interventional Radiology* **39** 1352–1357. (doi:10.1007/s00270-016-1350-1)

8 El-Maouche D, Sadowski SM, Papadakis GZ, Guthrie L, Cottle-Delisle C, Merkel R, Millo C, Chen CC, Kebebew E & Collins MT 2016 68Ga-DOTATATE for tumor localization in tumor-induced osteomalacia. *Journal of Clinical Endocrinology and Metabolism* **101** 3575–3581. (doi:10.1210/jc.2016-2052)

9 Haeusler G, Freilinger M, Dominkus M, Egerbacher M, Amann G, Kolb A, Schlegel W, Raimann A & Staudenherz A 2010 Tumor-induced hypophosphatemic rickets in an adolescent boy: clinical presentation, diagnosis, and histological findings in growth plate and muscle tissue. *Journal of Clinical Endocrinology and Metabolism* **95** 4511–4517. (doi:10.1210/jc.2010-0543)

10 Nasu T, Kurisu S, Matsuno S, Tatsumi K, Kakimoto T, Kobayashi M, Nakano Y, Wakasaki H, Furuta H, Nishi M, *et al*. 2008 Tumor-induced hypophosphatemic osteomalacia diagnosed by the combinatory procedures of magnetic resonance imaging and venous sampling for FGF23. *Internal Medicine* **47** 957–961. (doi:10.2169/internalmedicine.47.0745)

11 Ogura E, Kageyama K, Fukumoto S, Yagihashi N, Fukuda Y, Kikuchi T, Masuda M & Suda T 2008 Development of tumor-induced osteomalacia in a subcutaneous tumor, defined by venous blood sampling of fibroblast growth factor-23. *Internal Medicine* **47** 637–641. (doi:10.2169/internalmedicine.47.0761)

12 van Boekel G, Ruinemans-Koerts J, Joosten F, Dijkhuizen P, van Sorge A & de Boer H 2008 Tumor producing fibroblast growth factor 23 localized by two-staged venous sampling. *European Journal of Endocrinology* **158** 431–437. (doi:10.1530/EJE-07-0779)

13 Ito N, Shimizu Y, Suzuki T, Saito T, Okamoto T, Hori M, Akahane M, Fukumoto S & Fujita T 2010 Clinical utility of systemic venous sampling of FGF23 for identifying tumours responsible for tumour-induced osteomalacia. *Journal of Internal Medicine* **268** 390–394. (doi:10.1111/j.1365-2796.2010.02262.x)

14 Kuo R, Panchal M, Tanenbaum L & Crues JV III 2007 3.0 tesla imaging of the musculoskeletal system. *Journal of Magnetic Resonance Imaging* **25** 245–261. (doi:10.1002/jmri.20815)

Received in final form 20 February 2017
Accepted 10 March 2017